A controlled recipient evacuation process to form composite profiles from flat multi-angle prepreg stacks – infrastructure and C-profile verification

E. Kappel & M. Albrecht

Published online: 06 Sep 2019.

Submit your article to this journal ⤤

Article views: 20

View related articles ⤤

View Crossmark data ⤤

Taylor & Francis
Taylor & Francis Group

A controlled recipient evacuation process to form composite profiles from flat multi-angle prepreg stacks – infrastructure and C-profile verification

E. Kappel and M. Albrecht

DLR, Institute of Composite Structures and Adaptive Systems, Braunschweig, Germany

ABSTRACT

Single-diaphragm forming is a cost saving alternative to labor-intensive ply-by-ply layup. This paper reports on forming of flat uncured multi-angle prepreg stacks into C shape. The main focus is on the forming-process profile $p_{recipient} = f(t, T)$, which has attracted little attention in previous studies on the topic. Hexcel's M21E/IMA prepreg is examined within the study to analyze the particular effect of the prepreg's interleaf layers on the forming process and vice versa. Specimens with different multi-angle stackings were formed at 40, 60 and 80 °C, on male tools with 4, 6 and 8 mm radii. It is shown that the composed infrastructure setup allows for a precise control of the recipient pressure profile. The forming status is monitored based on a resistance-measurement-based approach, whose application suggests a two-phase forming process characteristic. Recipient pressure levels of 60 and 510 mbar below ambient pressure were identified as practical for gentle forming. It could be shown that interleaf layers of M21E/IMA specimens are not harmed considerably by the forming procedure. Overall, the proposed forming process led to prepreg preforms of adequate quality, suitable for series production.
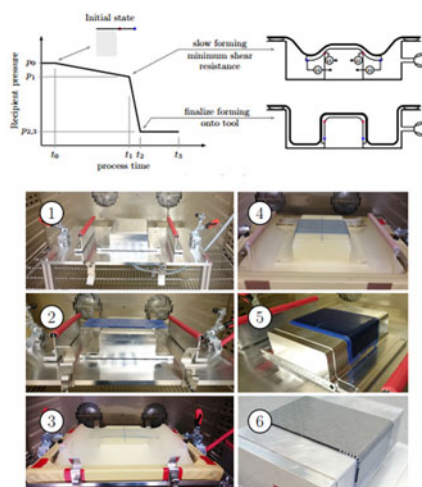
GRAPHICAL ABSTRACT
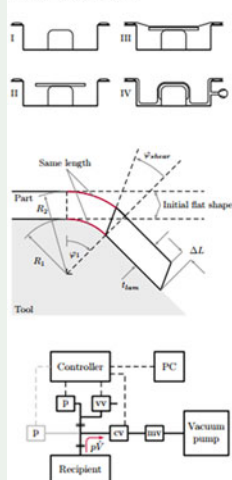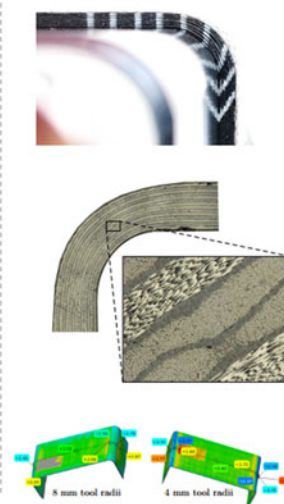
1. Introduction

Reducing manufacturing costs for composite structures is a key aim among OEMs in aerospace industries. While large structures of moderate curvature, such as wing and fuselage skins, are already made with ATL (automated tape laying) and AFP (automated fiber placement) technologies [1–3], many structural components, as for example stringers, spars and circumferential frames, are typically made in manual hand-layup processes, in which highly trained workers compose laminates ply-by-ply.

Unfortunately, those manually fabricated parts dominate aerospace assemblies in terms of numbers. For example, a side shell section 16–18 of an Airbus A350 XWB, comprises only a single skin, around sixteen circumferential frames, around thirty stringers (positions covered by multiple stingers) and

more than 350 clips [1]. As another example – the composite wing of a new short range airplane, discussed at Airbus, will require around 22,000 m of manufactured T-stringers per month in order to realize the aspired production rate of 60 aircrafts per month [4]. These scenarios indicate the strong demand for novel, faster composite manufacturing technologies, preferably with a higher level of automation and reduced costs.

Hotforming, which is used synonymously for single-diaphragm forming and hot drape forming in this paper, is suited to address the aforementioned demands [5]. It denotes the forming of initially flat uncured prepreg laminate stacks into non-flat shape. Forming takes place at elevated temperature of up to 80 °C, while the resin remains in a pre-gelation phase. The technique is applied here for the sake of a prepreg-preform creation, which are cured in conventional autoclave processes afterwards.

The present paper is focused on hotforming of flat laminate stacks into a C-shape profile, as shown in Figure 1. The research pursues the aim to evaluate the suitability of the hotforming approach by macroscopically assessing the preform quality. However, the main focus of the study is on the definition of a precisely controlled evacuation process, which can be described as 'gentle' from a material perspective. An infrastructure setup is presented which provides adequate control of the recipient pressure, allowing for the definition of a two-phase forming process characteristic.

Hexcel's M21E/IMA unidirectional carbon-fiber-epoxy prepreg [6, 7] is examined in the present study in detail. A single layup has been created from Hexcel's 8552/AS4 [8, 9], and forming results of both prepreg systems are compared.

Both prepregs have different internal laminate architectures, which result from their deviating toughening concepts. In-fact M21E/IMA has discrete resin-rich interleaf layers, interspersed with insoluble thermoplastic particles. The comparison with 8552/AS4 aims to assess the effect of those interleaf layers on the forming process. The work presented in this paper pursues a pilot-study concept [10], focussing on selected parameters from the immense parameter space. The study was set up to provide answers to the subsequent questions.

- Can flat full-stack prepreg laminates be formed into C-shaped profiles, while the laminate quality remains satisfactorily in terms of gaps and wrinkles?
- How does the vacuum infrastructure need to be set up in order to allow for precise evacuation-process control?
- How does a gentle forming process look like?
- Are the interleaf-layers of M21E/IMA laminates harmed in corner areas by the forming process?
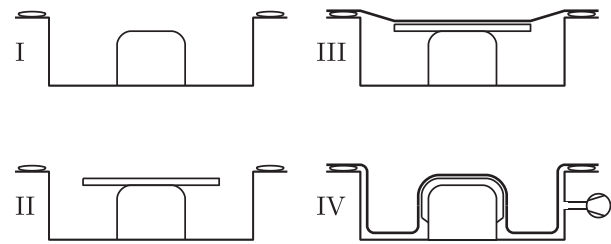

Figure 1. The investigated hotforming process.

- Does the hotforming process induce defects within the laminate architecture which can be identified in cured components?
- Does hotforming affect spring-in distortions of cured C-profiles in a technically relevant manner?

1.1. Previous relevant studies

Forming of initially flat full-stack prepreg laminates in non-flat geometries has been in focus of a limited number of studies. Those studies can be roughly distinguished in the subsequent groups.

- In-plane formability of different prepregs
- Wrinkle formation for non-developable surfaces due to ply-to-ply frictional interaction
- Numerical models addressing the forming process

Larberg et al. [11], investigated in-plane forming of different thermoset carbon-fiber epoxy prepreg systems, 977-2, 8552 and M21, based on the Bias Extension Test. The authors used a temperature chamber for their tests and covered a forming temperature range from 45 °C up to 90 °C. The authors provided the statement that 'M21 including particles has a significantly higher viscosity' compared to the other prepregs, which substantiates the presumption that interleaf-toughening significantly affects the forming process, which is investigated in the present paper. In a related study Larberg and Åkermo [12] characterized inter-ply friction for different generation prepregs, two without and two with particles. The authors reported considerably higher friction coefficients for materials with particles, which underline the particular effect of interleaf layers on the forming process addressed in the present work. The authors also indicate that a material with a higher friction might be better suited for robust forming processes, as uncontrolled slippage is minimized.

Hallander et al. [13] investigated the development of wrinkles for a C-channel geometry, which comprises a joggle area. Due to the joggle, the surface becomes non-develop-able, which in turn leads to wrinkling. Hallander et al. used a hot-drape-forming process with 977-2/HT prepreg stacks. Forming was conducted at a temperature of 65 °C, while the recipient evacuation process has not been further

described. In a related study Hallander et al. [14] extended their earlier work on forming of C-profiles. The authors analyzed the effect of inserting cuts and layup modifications on the formation of wrinkles. The forming process characteristic has not been varied.

Sjölander [15] complements the studies of his colleagues [11–14] and performed a numerical study on wrinkling mechanisms, which focuses on the C-profile geometry. The authors conclude that good predictions were found, considering when and where different kinds of wrinkles appear. Sun et al. [16] performed a study focusing on forming of flat laminates into a C-profile shape by using a double-sided diaphragm process. The authors mainly focussed on $[45, -45]_{4s}$ laminate stacking made from unidirectional T300 carbon-fiber-epoxy prepreg. Forming temperatures were varied between $30\,°C$ and $80\,°C$. The authors found a better surface quality for higher forming temperatures. Too high temperatures led to corner thinning, similar to the observation presented later in this paper. The authors used a constant, rather abrupt double-diaphragm forming strategy, with a vacuum pressure $0.1\,MPa$ ($p_{\text{recipient}} = 1\,bar$ below ambient) and a forming process-duration of 12 s.

Wang et al. [17] performed a study on improving the composite drape forming quality by enhancing inter-ply slip. Contrary to other studies, the concept was to use powders and thin veils at ply interfaces to reduce ply-to-ply friction, instead of increasing the forming temperature. The study was performed with unidirectional 8552/IM7 prepreg. Forming was performed at $40\,°C$ with a constant 12 s seconds forming process. Haanappel [18] performed comprehensive studies on forming of unidirectional thermoplastic composites. In his PhD thesis the acting distortion, respectively forming mechanisms of the stamp forming process are excellently outlined. Some of the described mechanisms are relevant for the investigated forming of unidirectional thermoset prepregs of the present study, as discussed later in Section 2.3.

Farnand et al. [19] conducted a study on forming of flat laminate stacks into C-shape as well. The authors examined unidirectional CYCOM 5320/T650-35 out-of-autoclave prepreg and investigated $[90, 45, -45, 0]_{is}$ (with $i = 2, 4, 8$) and $[0, -45, 45, 90]_{4s}$ layups. They performed forming at temperatures of $30\,°C$ and at $70\,°C$. Farnand et al. describe their forming procedure by a constant forming rate of $6.4°/s$ ($\approx 14\,s$ to form the $90°$ angle). Variations of the forming-process-characteristics were not executed.

Erland et al. [20] performed a comprehensive analysis on inter-ply shear properties for uncured 8552/AS4 prepreg. The authors developed a model which describes how temperature, forming rate and pressure affect the behavior of the prepreg during forming. The authors clearly showed that shear stress τ decreases with increasing shear strain γ when temperature increases from 40 to $90\,°C$. Erland et al. [20] also examined the effect of varying pressure levels on shear stress τ for a constant forming temperature of $90\,°C$. The results show clearly that a reduction of pressure significantly reduces the corresponding shear stress. These findings support the guiding idea of the present paper, which focusses on a controlled two-step forming process. The first step of this process is characterized by a small relative pressure magnitude, which should lead (according to [20]) to a minimum resistance against shearing. After shearing has migrated from the bends along the flanges, the second process step realizes the full forming onto the tool, by increasing the relative pressure between the recipient and the ambient conditions.

Bian et al. [21] published a comprehensive article on double-diaphragm forming of C-profiles using unidirectional Cytec X850 carbon-fiber-epoxy prepreg. The authors investigated the forming temperature at 45, 60 and $80\,°C$ and three different evacuation rates of 4000, 500 and 250 mbar/min for $[45, -45]_8$ layups.[1] They used pull-out tests to determine inter-ply friction properties. They measured considerable friction for forming at $45\,°C$, while almost identical, significantly lower values were determined for forming at $60\,°C$ and $80\,°C$. Macroscopic analyses of the created preforms revealed wrinkles at the preforms' inner tool-sided surfaces, whose appearance correlates with the observed inter-ply friction characteristics. Specimens formed at $45\,°C$ showed wrinkles close to the corner area, while specimens formed at $60\,°C$ and $80\,°C$ did not. Specimens, preformed at $45\,°C$ still showed wrinkles after autoclave curing on steel-male-molds. Differences of the inner laminate quality were not identified for preforms created at 50 and $60\,°C$. The effect of laminate-stacking, and in particular the effect of $0°$ and $90°$ layers, was not investigated.

The available studies provide valuable information on relevant forming temperature ranges and the effect of ply orientations, which is adopted for the study presented in this paper. However, the characteristics of the forming process, in terms of a profile of recipient pressure over time, were not investigated satisfactorily in the past. Successful forming requires slippage and shear, which in turn directly depend on the resin's viscosity, inter-ply friction and the pressure acting on the laminate. In particular the results of Erland et al. [20] indicate

---

[1]Note, Bian et al. used evacuation rates defined in kPa/min which equals 10 mbar/min.

Table 1. Parameters affecting the hotforming process.

Prepreg specific
Unidirectional or fabric reinforcement
Prepreg architecture (toughening)
Pre-curing state
Resin viscosity
Fiber volume fraction
Part specific
Laminate stacking sequence
Corner radii
Profile cross section geometries
Tooling specific
Tool surface properties
Tool material
Distance sheets
Forming membrane properties
Male or female tooling concept
Membrane pre stressing
Processing specific
Heat input concept
Temperature homogeneity
Forming speed
Recipient pressure profile
Pressure levels and dwell duration
Pre-compaction state of the laminate

M21E/IMA with interleaf toughening

Figure 2. Ply-to-ply interface of a M21E/IMA laminate with interleaf layer, containing thermoplastic particles.

2.1. Relevant parameters

A preliminary analysis of the forming process itself suggests a parameter clustering into the four categories 'Prepreg specific', 'Part specific', 'Tooling specific' and 'Processing specific'. The particular aspects of these categories are listed in Table 1. Selected parameters, as for example the forming tool radius as well as the laminate stacking sequence are varied in the present study.

2.2. Material properties

Hexcel's M21E/IMA prepreg was used, which is the reference prepreg for the Airbus A350 XWB. M21E/IMA is a 3rd-generation prepreg, which has insoluble thermoplastic particles at both ply surfaces [3]. These particles create inter-ply resin-rich layers within the laminate architecture, the so-called interleaf-layers. These particles act similar to spacers, known from adhesive applications. This particular prepreg material has not been analyzed in any of the available studies. A typical M21E/IMA laminate architecture is shown in Figure 2.

To assess the effect of those interleaf layers a set of $[45, 0, (90, -45)_2, 45]_s$ laminates has been formed from both, the aforementioned M21E/IMA prepreg and from Hexcel's 8552/AS4 prepreg. The latter is a 2nd-generation prepreg with dissolved toughening modifiers in the resin. 8552/AS4 prepreg has been used in an earlier study of Larberg [11]. The inner laminate architecture of both specimens is compared, to outline potential differences induced by the interleaf-layer laminate architecture.

2.3. Distortion mechanisms

According to Haanappel [18], the physical process during press forming (double-sided tooling) distinguishes into interface and intra-ply mechanisms. The former distinguishes further in tooling slippage and ply slippage, which is enabled by fluid shearing.
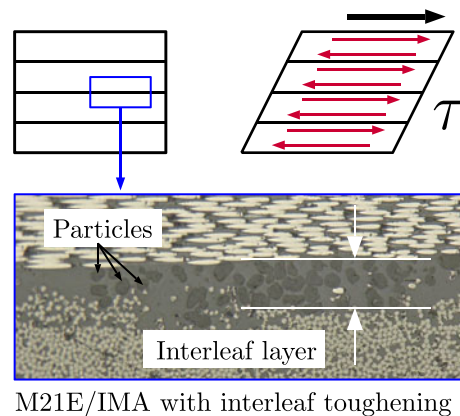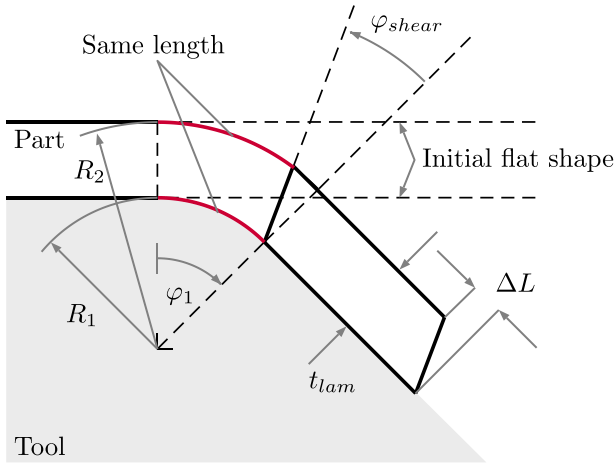
that better preform results are likely when pressure on the laminate during forming is limited. An appropriate control of the evacuation procedure is expected to create preforms of desired quality in a minimum of time. Thus, for the study at hand, the design of the evacuation process is the key parameter in focus. The rather low geometric complexity of the C-profile has been chosen, in order to avoid blurring of results due to superposing affectations, such as wrinkling as a consequence of a non-developable part geometry.

1.2. Promising applications

The present study analyzes forming of flat multiangle laminate stacks into a C-profile shape. This represents a developable surface, in particular a linearly extrusion with a constant cross section. Many composite parts in recent composite-dominated fuselage designs show similarities to the structure in focus, as for example wing ribs, stringers, circumferential frames, inter-coastals, clips, cleats, brackets, struts, floor- and cargo beams as well as wing spars. The paper at hand should provide new insight, allowing for the adoption of hotforming to the aforementioned structural components, which will be presented in a related article.

2. The hotforming process

Forming a flat laminate stack into a C-profile shape represents the lowest geometrical complexity increase. Nonetheless, the number of process- and material-related parameters, which affect the outcome, is immense. This section outlines the most relevant parameters and provides an idealized geometric model to describe an ideal forming process.

Figure 3. Geometric relations during forming. Note, that laminate thickness reductions are not considered in the simple model.

Delamination due to ply separation is also conceivable. Intra-ply mechanisms are further distinguished in longitudinal and transverse intra-ply shear, as well as fiber tension and ply bending. It should be noted that not all mechanisms are relevant for the forming process regarded in the study at hand, as in contrast to Haanappel a single-sided tool concept combined with a single membrane is used here. However, an interaction of the membrane and the laminate stack is assumed during forming, even though release film layers are utilized to minimize it. As the membrane exhibits considerable strain during the forming process, an interaction with the adjacent layers is enforced with increasing pressure difference between the recipient and the ambient air. For the study at hand the interface effect of inter-laminar ply slippage is considered as the dominant mechanism.

3. A simple geometrical model

Simple geometrical analyses allow for the calculation of an idealized shear angle, which arises when an initially flat laminate stack is formed around a positive tool corner. Figure 3 shows the corresponding geometric model. R_1, φ_1, t_{lam} denote the male tool-corner radius, the sector angle and the laminate thickness, respectively. ΔL denotes the maximum step length induced by the forming. Wang et al. [17] denotes this shape as book-end effect.

ΔL results from the sector length differences between the inner and the outer layers of the curved part area which arise as all plies initially had the same length in the flat state. Both sector lengths are given by

$$S_1 = R_1 \cdot \varphi_1 \quad \text{and} \quad S_2 = R_2 \cdot \varphi_1. \qquad (1)$$

With, $R_2 = R_1 + t_{lam}$ it follows that

$$\Delta L = S_2 - S_1 = t_{lam} \cdot \varphi_1. \qquad (2)$$

Therefrom, the laminate shear angle is derived, which is used for evaluation purposes:

Table 2. Applied model parameters for the cure kinetic [22] and the viscosity [23] models for the 8552 resin system.

Cure model	Viscosity model
$m = 0.813$	$A_\eta = 3.25 \times 10^{-10}$ Pa s
$n = 2.74$	$E_\eta = 7.654 \times 10^4$ J/mol
$K = Ae^{\frac{-\Delta E}{RT}}$	$\alpha_g = 0.47$
$C = 43.1$	$A = 3.8$
$\alpha_{C0} = -1.684$	$B = 2.5$
$\alpha_{CT} = 5.475 \times 10^{-3}$ 1/K	–
$\Delta E = 66.5$ kJ/(g mol)	–
$A = 1.535 \times 10^5$ 1/s	–
$R = 8.314$ J/(mol K)	$R = 8.314$ J/(mol K)

$$\varphi_{\text{shear}} = \arctan\left(\frac{\Delta L}{t_{\text{lam}}}\right) = \arctan\left(\frac{\varphi_1 \cdot \pi}{180°}\right) \qquad (3)$$

φ_{shear} is found independent from the part radius and from the laminate thickness. For a 45° or 90° sector angle, φ_{shear} is calculated to 38.1° or 57.5°, respectively. As will be seen in Section 5.1, the latter value matches the observations during the experiments quite well. Variability of the shear angle in through-thickness direction indicates deviations from the ideal forming process, as for example first-ply wrinkling outlined by Farnand et al. [19].

4. Experimental study

4.1. Preliminary analyses

Johnston's [22] CHILE[2] cure-kinetics is used here to assess whether a significant increase of the degree of cure α needs to be expected during the forming process. This is essential information since in today's processes it is a requirement that layup composition should not affect the resin's degree of cure. The applied cure-kinetics model is given in Equation 4.

$$\frac{d\alpha}{dt} = \frac{K \cdot \alpha^m \cdot (1-\alpha)^n}{1 + e^{C\left(\alpha - (\alpha_{C0} + \alpha_{CT} \cdot T)\right)}} \qquad (4)$$

The obtained degree of cure $\alpha = f(t)$ data is subsequently used to determine the resin's viscosity during the forming process, while the viscosity model of Hubert [23] is used, which is given by Equation 5.

$$\eta = A_\eta \cdot e^{E_\eta/RT} \cdot \left[\frac{\alpha_g}{\alpha_g - \alpha}\right]^{A + B\alpha} \qquad (5)$$

As corresponding model parameters are unavailable for the M21E resin, and a determination was out of scope of the performed pilot study, the analysis was performed for the 8552 resin only. The utilized resin parameters are summarized in Table 2. They are provided in Johnston [22]. The following analysis considers the lower temperature threshold

---

[2]CHILE denotes cure-hardening-instantaneous-linear–elastic.
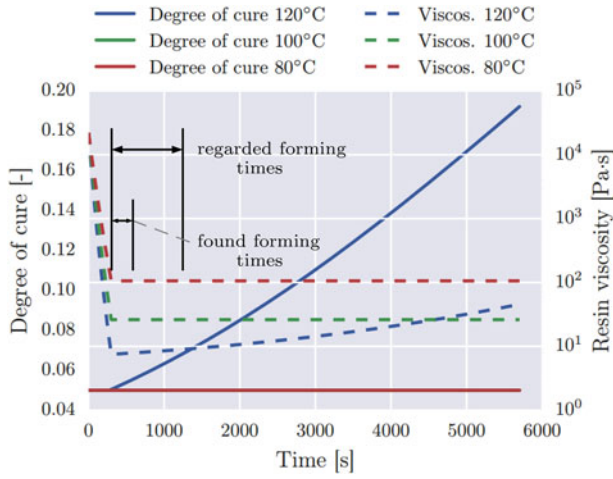
Figure 4. Degree of cure and viscosity development for the 8552 resin. Note that no degree of cure increase is predicted for the 80 °C and the 100 °C process.

of 80 °C which has been captured during the experiments. The forming process comprises a rather abrupt heating from room temperature (25 °C) to the maximum forming temperature within 5 min, followed by a dwell stage at that temperature. The heating profile mimics the positioning process of the flat prepreg stack on the pre-heated forming tool, while the second period captures the forming process itself. The degree of cure and the resin viscosity are analyzed. A 90-minute dwell period is considered at 80 °C, 100 °C and 120 °C, in order to identify at which temperature an increase of the resin's degree of cure needs to be expected. The analysis represents a worst-case scenario, since the present experimental study utilizes lower temperatures between 40 °C and 80 °C and shorter dwell periods. As no relevant increase of the degree of cure was found for forming up to 80 °C the analysis aim was shifted in order to identify at which forming temperature the onset of a degree of cure increase must be expected.

Figure 4 shows that even for a rather high forming temperature of 100 °C the resin's degree of cure is not increased during a rather long forming process. For the lower threshold of the regarded temperature range a resin viscosity of around 100 Pa· s is derived, which is reasonable according to the resin's data sheet [9]. The analysis revealed that the selected upper temperature threshold of 80 °C for the real forming process is a reasonable choice when it is a given requirement that the resin's degree of cure should not be elevated during the forming process. As can be seen in Figure 4, forming at 120 °C will lead to an increase of the resin's degree of cure.

4.2. Hotforming infrastructure – vacuum setup

Figure 5 shows the setup used for the hotforming experiments. A Vacuubrand CVC 3000 vacuum
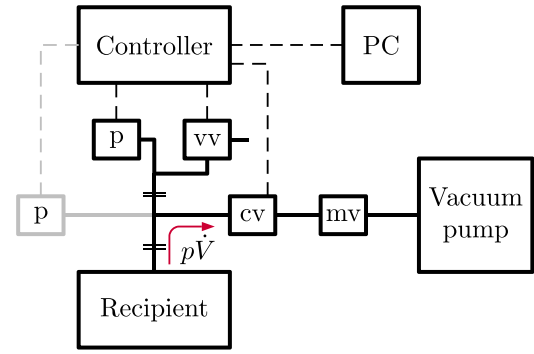
Figure 5. Schematic of the used vacuum infrastructure. p, cv, vv, mv denote pressure sensors, a controlled valve, a ventilation valve and a manual valve, respectively. Dashed lines indicate data lines. Light gray elements have been used for reliability reasons and = indicate ball valves.

controller [24] was used to control the recipient pressure during the process. It has a control range from 0.1 mbar up to 1080 mbar. The controller has an internal pressure sensor (p) whose signal is used as input for the controllable valves (cv) and the ventilation valve (vv). For reliability reasons an external pressure sensor is used in parallel. A manual valve (mv) is used to limit the volume flow towards the vacuum pump. This volume-flow limitation was mandatory to realize a robust control, as the recipient volume in the study is comparably small and the throughput of the vacuum pump comparably high. The controller is connected to a PC via an RS232 port for sake of data acquisition and programming. A python-based routine has been created to transfer user recipient-pressure profiles from the PC to the controller. It allows for the prescription of evacuation profiles based on (t_i, p_i) data points or gradient definitions $(\Delta t_i, \Delta p_i)$.

4.3. Hotforming infrastructure – tooling

Figure 6 shows the tooling infrastructure used throughout the present study. Basically, the bottom part contains an aluminum base plate, two distance plates, two holding clamps, four holding springs, four stands and the aluminum C-profile male tool. The vacuum port is positioned centrally underneath the tool, which itself is mounted to the base plate. Washers were used, in order to provide a small gap between the tool and the base for evacuation purposes. The frame of the forming tool's upper part is made from conventional aluminum profiles. A low temperature latex membrane with maximum elongation of 850% has been used [25]. The membrane is wrapped around the frame and clamped in position. Six aluminum C-profile tools were available in total (2×4 mm, 2×6 mm and 2×8 mm male radii), which allows for simultaneous curing of multiple parts in a single autoclave run, subsequent to the
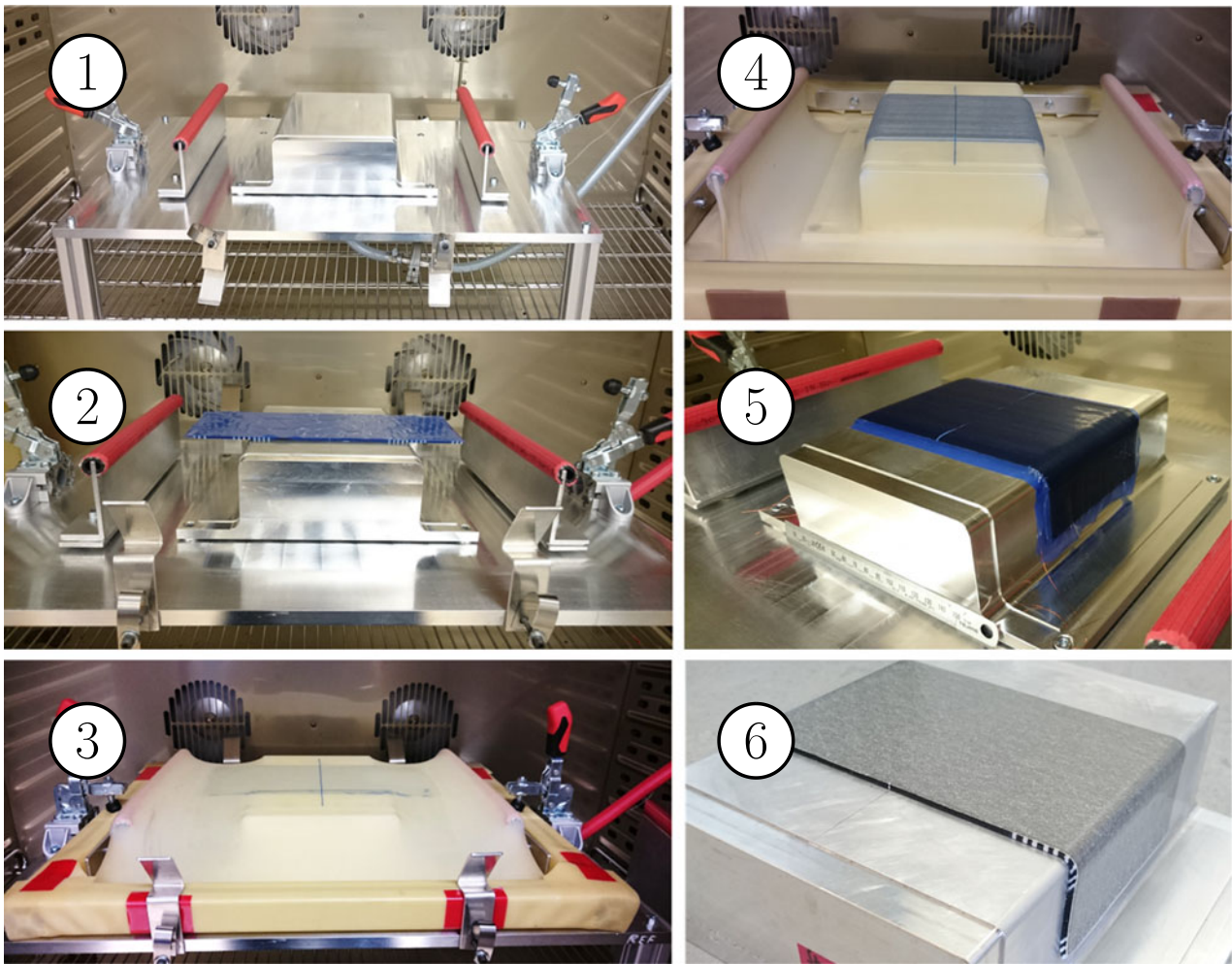
Figure 6. Hotforming infrastructure and specific process steps.

forming process (see Figure 18). Figure 6 shows the six states during the forming process.

1. Tooling prepared and heated to forming temperature
2. Flat laminate stack positioned on the tool
3. Upper tool with membrane applied
4. Evacuation process finalized
5. Upper tool removed
6. Curing process finalized

### 4.4. Forming process characteristics

The definition of an applicable and preferably simple forming-process characteristic is the main objective of the study. In particular, the identification of a parameter set comprising the temperature during forming and the recipient pressure control over time was in focus. Forming temperatures of $40\,°C$, $60\,°C$ and $80\,°C$ are investigated in the present study, similar to study of Bian et al. [21] who investigated temperatures between 45 and $80\,°C$. The evacuation characteristic for a certain scenario depends on the vacuum infrastructure at hand as well as on the recipient's specifications. Thus, only limited information could be directly adopted from the literature to the scenario at hand.

Thus, preliminary tests have been performed to define characteristic states during forming. Laminate stacks with different stacking sequences were formed using the described tooling infrastructure. Observations during these tests reveal a very similar forming procedure for all inspected laminates. Figure 7 shows a schematic of the observed distortion mode during forming.

The exact times where local contact between the part and the tool is established, were determined using resistance measurements. Therefore, thin uncoated copper wires were applied on the flat laminate stacks. During forming the electrical resistance between the tool and the wires was measured. A sudden drop in resistance during the process was interpreted as the time when tool-part contact is established. These tests were used to define the initial forming-process characteristic, which is shown in Figure 7. It was found that the red wires establish a contact with the tool early on in the process, indicating that forming at the bend areas is finished at recipient pressure levels close to ambient condition. Due to the small pressure
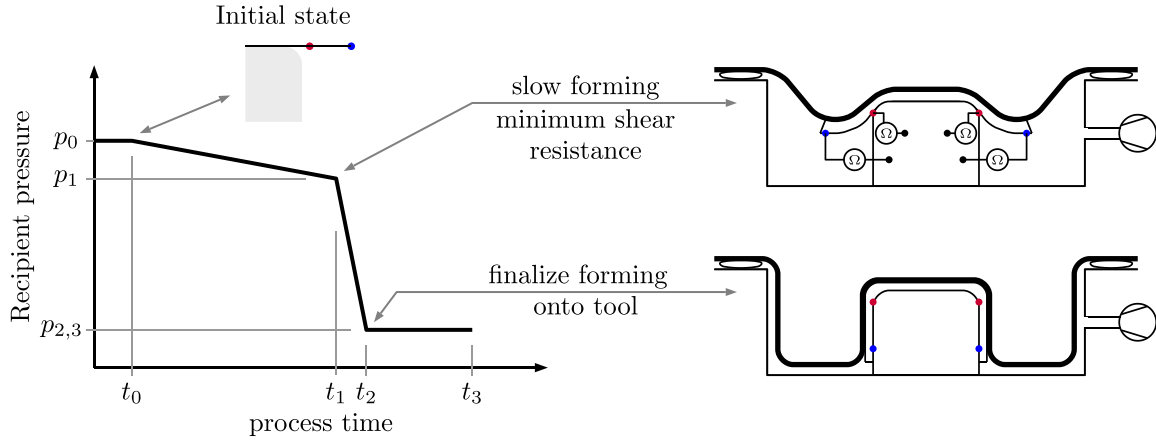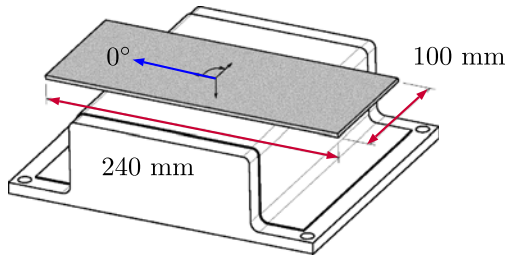
Figure 7. Typical distortion states observed during forming (right) and corresponding recipient pressure levels (left). Red and blue dots indicate inner and outer copper wires. respectively, which have been used to characterize the forming procedure. $p_0 = p_{ambient}$.
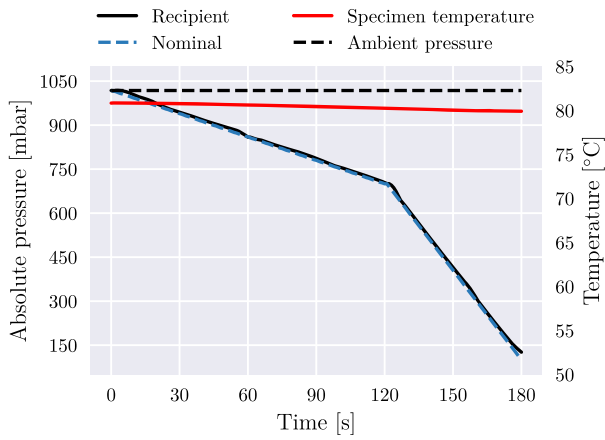
Figure 8. Nominal and realized example evacuation process, for an $80\,°C$ forming process with $t_2 = t_3$ and $p_{2,3} = 150$ mbar.

Table 3. Layup configurations.

ID	Layup	Prepreg
L1	$[(90,0)_3,90]_s$	M21E/IMA
L2	$[(0,90)_3,0]_s$	M21E/IMA
L3	$[0_7]_s$	M21E/IMA
L4	$[45,-45,0,(-45,45,0)_2,45,-45,0,-45,45]$	M21E/IMA
L5	$[45,0,-45,0,45,0,-45]_s$	M21E/IMA
L6	$[45,-45,90,(-45,45,90)_2,45,-45,90,-45,45]$	M21E/IMA
L7	$[45,90,-45,90,45,90,-45]_s$	M21E/IMA
L8	$[45,0,(90,-45)_2,45]_s$	M21E/IMA
L8*	$[45,0,(90,-45)_2,45]_s$	8552/AS4

nominal recipient pressure profile and the measured profile was observed. Figure 8 shows an example, which verifies that the utilized infrastructure is capable of providing the desired process conditions.

4.5. Curing process

After the preforming process is finalized, the formed laminate M21E/IMA stacks are cured within a conventional autoclave process. The MRCCs is used which has final curing temperature of $180\,°C$ [9]. Process-induced distortions of the cured C-profiles are evaluated as well in order to compare the obtained distortion with results of previous studies on C-profiles [26] which have been manufactured with a manual ply-by-ply layup. This provides insight whether hotforming affects process-induced distortions of composite structures.

4.6. Laminate configurations

The present study focusses on 14-ply laminates, which is due to project boundaries and the necessity to limit the number of specimen configurations. The reference ply-stack dimensions, the laminate's $0°$ direction and the used C-profile tool are shown in Figure 9. The examined laminate configurations are listed in Table 3.

Figure 9. Laminate stack dimensions, the laminate's $0°$ orientation and the used tools for forming and curing.

difference only little pressure is acting on the laminate stack, which leads (according to Erland et al. [20]) to a minimum resistance of the material against shearing. However, the little pressure difference is not capable to form the full laminate stack onto the tool. A force equilibrium is observed, similar as shown in Figure 7 (top right). Thus, the recipient pressure is further reduced to fully form the laminate stack onto the tool surface, as shown in Figure 7 (bottom right).

Vacuum infrastructure tests were conducted, until a satisfying match between the prescribed

Table 4. Corner points of the preliminary forming process.

Time t in [min]	Recipient pressure p in [mbar]
$t_0 = 0$	$1010 \approx p_{ambient}$
$t_1 = 20$	950
$t_2 = 25$	500
$t_3 = 30$	500

Figure 10. Shear angle development along the corner of a specimen with L2 layup.

Figure 11. Laminate run-out areas. L8 laminate formed at 80 °C (left) and 40 °C (right).

Figure 12. Laminate run-out areas for M21E/IMA (top row) and 8552/AS4 (bottom row) specimens, both with $[45, 0, (90, -45)_2, 45]_s$ layup.
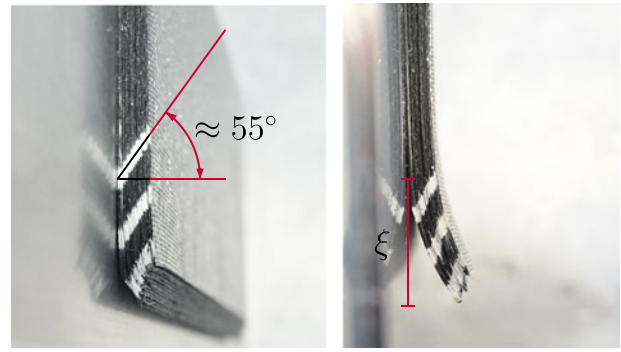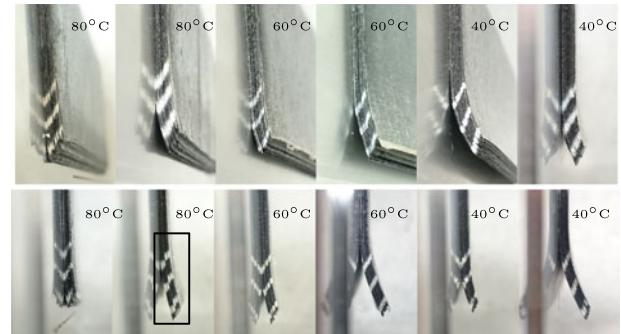
5. Results

5.1. C-channel forming process

The introduced test setup (Section 4.4) has been used to determine characteristic states during the forming process. Within preliminary forming the recipient pressure was manually reduced until contact between the copper wires and the tool was detected. Unidirectional layups have been used for these tests, in order to account for the highest conceivable laminate bending stiffness of the examined laminates. The first test served to define preliminary pressure levels of the forming process. A forming temperature of 60 °C was used, which is centrally in the forming-temperature range investigated by Bian et al. [21]. The authors measured comparable inter-ply friction for 60 °C and 80 °C tests, while significantly higher inter-ply friction was found for forming at 45 °C. Thus, 60 °C represents the economic choice, promising a wrinkle-free forming and little affectation of the resin's degree of cure.

A second test serves to determine corresponding time intervals. For the configuration at hand first contact of the inner wires (red dots in Figure 7) is observed between 940 and 950 mbar recipient pressure, while the initial ambient pressure was 1010 mbar. Stable contact of the outer wires (blue dots) is observed at a recipient pressure of 650 mbar, only 360 mbar below ambient pressure.

It should be noted that those pressure values represent a first data set to define a controlled forming process. Those are valid for the configuration at hand only. In fact, different levels are likely when

laminate properties or essential components of the forming infrastructure change, as for example the membrane type or the setup/part dimensions. Nonetheless, due to the limitation to 14-ply laminates and the fact that the forming infrastructure remains constant throughout the study, the determined values prove suitable during the forming trials. The initial reference process was defined as given in Table 4. The identified process time is rather long compared to processes investigated in other studies (see e.g. Farnand et al. [19]). However, the study concept adopted here is to start from the most conservative process, which showed satisfying forming results and reduce process time successively until first laminate flaws are observed. In any case it is believed that the laminate architecture benefits from longer forming times, as the resin viscosity is rather high during forming. Later in this study, shorter processes were used, as for example a 3-minute process shown in Figure 8.

5.2. Preform quality – macroscopic analysis

A white line pattern, sprayed on the side faces of the C-specimens, has been utilized to assess the shear distortions of the laminate (see Figure 10). The patterns have been applied to the flat laminate stacks, particularly at the bend and at the part's
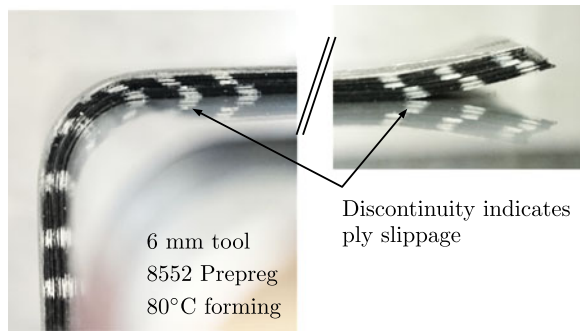
Figure 13. Ply-to-ply slipping observed for selected 8552/AS4 specimens.
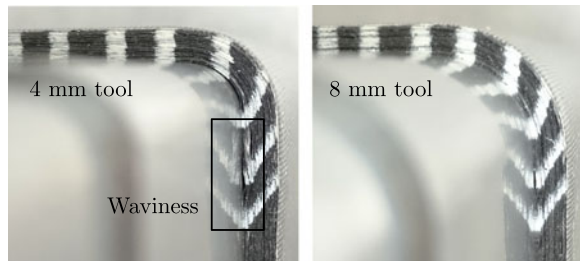
Figure 14. Effect of tool radius for M21E/IMA specimens with L8 layup.

run-out areas. Figure 10 shows an example, where an L2 laminate has been formed at 40 °C. Figure 11 shows two different laminate run-outs. While some laminates fit the tool completely at the end of the forming process, others show areas which stay away from the tool, as can be seen in Figure 11. The measure ξ is introduced to quantify and assess the forming result. The observed shear angle (book-end effect) at the laminate run out shown in Figure 11 (left), matches quite well with the estimation of 57.5°, provided by the simple model given in Section 3.

The majority of the specimens showed no or only little flaws. None of the observed flaws is considered to affect the parts performance negatively in a technically relevant extent. Nonetheless, the observed effects are outlined subsequently.

Figure 12 shows laminate-run-out areas for both prepreg systems (L8 stacking). The same trend can be identified for both systems. A higher forming temperature improves the forming result, as the ξ area is minimized. The analysis of the spray patterns indicates a continuous distribution of the shear angle in through thickness direction for the M21E/IMA laminates. Selected 8552/AS4 specimens show forming discontinuities, as highlighted in Figure 12 (bottom row).

Discontinuities indicate ply slippage. Figure 13 shows that the slippage is initiated in the bend area, while the discontinuity is already fully developed at the bend-to-flange transition. M21E/IMA specimens did not shows ply slippage, which can be a consequence of the higher inter-ply friction due to the particles on the plies' surfaces as indicated by Larberg and Åkermo [12]. However, as slippage is not accompanied by wrinkling, a detrimental affectation of the laminate architecture is unlikely.

The male-tool radius has been considered a particularly critical parameter in advance of the present study. A small radius reduces the laminate area in which the full shearing angle needs to be established.

Selected specimens substantiate this concern, as it is shown in Figure 14. Specimens, formed on a 4 mm male tool showed a slight trend to fiber waviness in laminate areas adjacent to the tool surface. Bian [21] reported on a similar observation, as they also found wrinkles close to the bend area of the inner part surfaces. However, other specimens formed on 6 and 8 mm tools and even others formed on the 4 mm tool did not show this effect. Additional tests and test repetitions are mandatory in order to analyze whether a technological limit must be expected when tool radii are in the range of 4 mm and smaller. Fiber waviness effect is considered the most critical of the outlined, as the introduced waves will persist after curing, leading to a decrease of mechanical performance.

5.3. Laminate architecture – microscopic analysis

Micro sections were created from the corner areas of the cured C-profiles. Those are used to assess the integrity of the internal laminate architecture after curing. The analyses focus on identifying obvious flaws and abnormalities, as gaps, overlaps or a critical damage of interleaf layers for example. A statistical analysis on the probability of occurrence could not be performed due to the pursued one-specimen-per-configuration concept. Figure 15 shows representative examples for both prepregs systems. The interleaf layers can be clearly seen for the M21E/IMA specimens. The micro-section analyses substantiate that the hotforming process does not harm the general interleaf-layer laminate architecture.

Selected specimens, with the L1 layup, show little trends for fiber migration in 90°–90° ply-sequences, as can be seen in Figure 16.

5.4. Towards the optimal forming process

Supported by the observations from the preliminary forming tests a bi-stage evacuation process is pursued as shown schematically in Figure 7. Each stage is characterized by a specific instantaneous recipient pressure level. For the tests at hand two-thirds of the total forming process is allocated to linearly approaching the first pressure level, while the
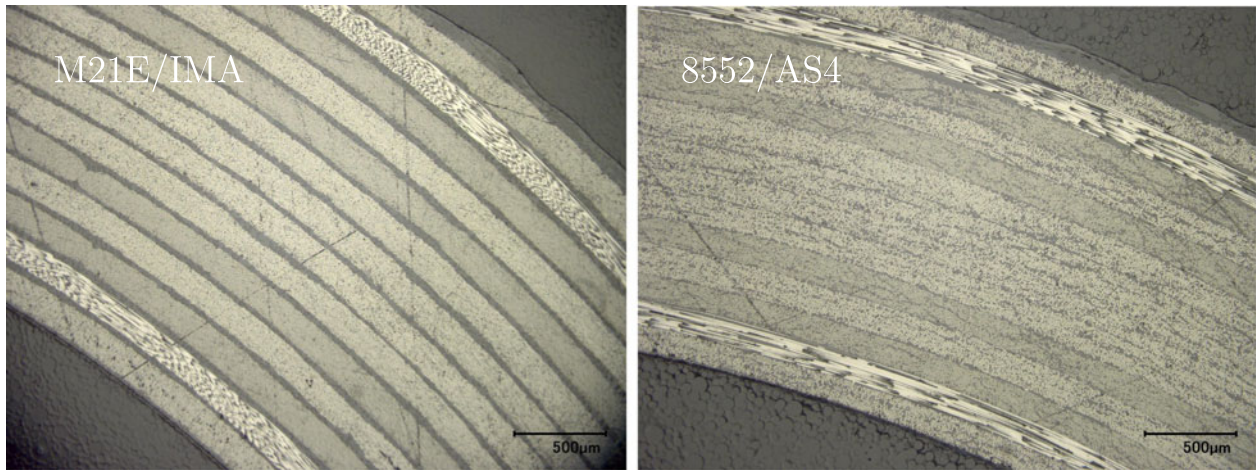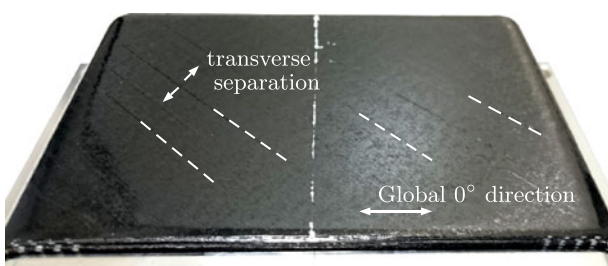
Figure 15. Flawless micro sections of curved laminate areas from M21E/IMA (left) and 8552/AS4 (right) prepreg. The straight lines in both pictures refer to the micro-section grinding/polishing process and do not represent laminate flaws.
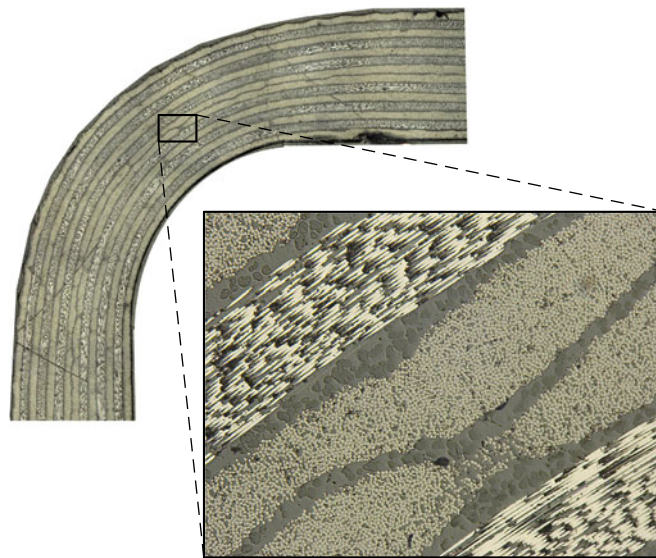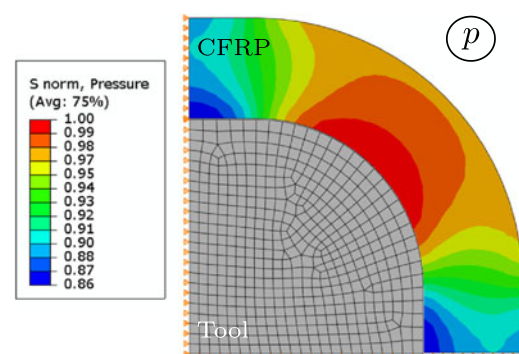

Figure 16. Flaws observed in 90°–90° ply sequences of the M21E/IMA laminates.

Figure 17. Flaws observed at the prepreg-membrane interface after forming (prior curing). Dashed lines indicate ply-separation in transverse direction.


Figure 18. Simultaneous curing of multiple prepreg preforms in a single autoclave run.

Figure 19. Normalized pressure gradient at part bend. p denotes the autoclave pressure. $S, \text{Pressure} = -\sigma_{ii}/3$ and 'S norm, Pressure' is defined as $\frac{-\sigma_{ii}}{3 \cdot \max(S, \text{Pressure})}$.

remaining third is allocated to approaching the second pressure level. This distribution is based on the conception that early on in the forming process, until the first pressure level is reached, the shear-angle has to develop homogeneously and almost instantaneously at the bend area and the flanges.
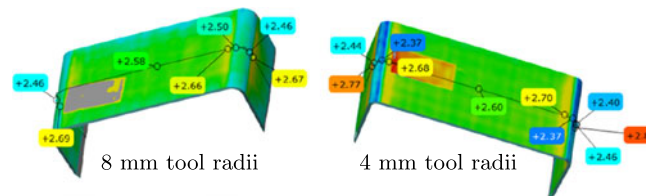
Figure 20. Example thickness evaluation of cured C-profiles. Rectangular zones on the web represent specimen-marker stickers.

Since this phase of the process is considered most relevant for a successful forming the better part of the forming process time is allocated for it.

5.5. Infrastructure related defects and counter measures

Most of the laminates formed in the present study showed acceptable inner-laminate-architecture quality. However, flaws at the web area of the C-profiles were identified for selected configurations. Those are either related to a specific laminate architecture at hand or to the particularities of the applied forming procedure. Figure 17 shows an example for a specimen with an outer ply oriented in $45°$ direction.

Inter-fiber separation in the ply's in-plane transverse direction is observed. Comparisons between different laminate configurations indicate that this separation is also affected by the ply underneath the outermost ply. Slightly higher separation was observed for a laminate with a subsequent $-45°$ ply in comparison to a configuration with a subsequent $0°$ ply. This is likely induced by the supporting effect, related to the fiber-direction of the ply underneath. However, additional test repetitions are required to further substantiate this indication.

The separation effect itself is considered a consequence of the interaction between the membrane and the outer ply. The membrane experiences considerable in-plane tension during forming as its area dimensions increase as shown in Figures 1 and 6-④. Simultaneously, the difference between the recipient pressure and the ambient pressure induces normal forces, which enforce a mechanical interaction between the membrane and the laminate stack. At the point when the stack is formed the stiffness of the plies in transverse direction is close to its minimum (resin dominated), due to the elevated temperatures. The uppermost ply tends to follow the stretching membrane, which results in the observed inter-fiber separation in transverse direction, leading to gaps shown in Figure 17.

Gaps between tows are critical from a structural-performance perspective, which has been intensively investigated in context of AFP processes [27]. After

autoclave curing, those gaps are filled with neat resin. However, if gaps are too large, they lead to stress-concentrations within the laminate which promotes failure. Lan et al. [28] named a critical gap-width threshold of 1.0 mm. Sawicki and Minguet [29] determined a threshold of 0.762 mm. The gaps observed in the present study were significantly smaller than the aforementioned thresholds. Thus, they are considered irrelevant from a structure-performance perspective.

In addition, the observed separation effect could be completely circumvented by adding 0.066 mm thick E-glass fabric layers (e.g. HexPly-M1080, [30]) on both sides of the flat carbon-fiber laminate stacks. As those layers are used by default for pre-preg-based airframe components for sake of electro-chemical shielding, the requirement for those extra plies isn't considered a detrimental aspect of the forming process. Instead it is concluded that a series-type layup even shows an improved forming behavior.

5.6. Spring-in analysis

Spring-in distortions come to light after a part is cured. Hence, the assessment of the forming-process-induced effect on spring-in is only possible when part parameters, as for example the corner radius R, do not induce any additional variances related to the autoclave processing itself. For the single-sided, male-tool manufacturing process, used throughout this study (see Figure 18), this requirement could not be fulfilled, as an effect of the corner radii was observed.

Laminate thickness evaluations on cured specimens revealed a linearly decreasing trend between the laminate thickness reduction at corner areas and the part's corner radius, as exemplary shown in Figure 20. The effect is typically denoted as corner-thinning, which is a consequence of the different dimensions of the part's inner surface, which is in contact with the tool, and the part's outer surface, which is subjected by the autoclave pressure. This difference results in an internal pressure gradient which initiates and enforces resin migration (see [31]). A simple qualitative FE model, shown in
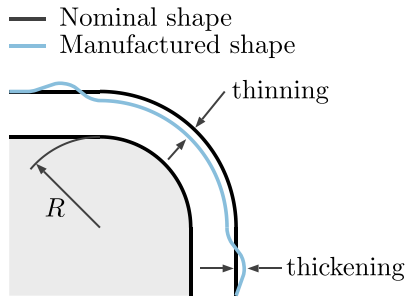
Figure 21. Observed corner thinning.

Figure 19, illustrates the normalized pressure distribution at the part's bend. Resin migrates from high-pressure areas into low-pressure areas until equilibrium is achieved.

During the curing process of the C-specimens, resin squeeze was prevented in the manufacturing setup by use of edge dams. It was found that corner thinning is accompanied by local laminate thickening at both sides, adjacent to the bend areas, which can be seen in the full-field scans of manufactured parts shown in Figure 20.

Figure 21 shows a schematic of the observed cross-sectional shape, indicating the thickness reduction at the bend and the accompanying laminate thickening beside it.

Even though a clear relation between spring-in and the hotforming procedure could not be developed, spring-in angles have been quantified. The results provide valuable insight, as a quantitative relation between corner thinning and spring-in distortions could be shown. The results substantiate the analytically outlined relation of a decreasing spring-in magnitude for increasing fiber-volume fractions [32]. Corner thinning between 0.08 and 0.28 mm has been found for the analyzed M21E/IMA C-profiles.[3]

The smaller the tool radius, the higher the local laminate-thickness reduction at the bend. Higher thickness reduction is equivalent to more resin flow. This is equivalent to a local increase of V_f and consequently a reduction of spring-in. For the M21E/IMA specimens at hand the local fiber-volume fraction V_f changes as followed. The 14-ply laminate has a nominal laminate thickness of 2.64 mm. For a V_f of 59%, around 1.08 mm of the laminate thickness is allocated by resin. Thus, the observed corner thinning (laminate-thickness reduction) of 0.08–0.28 mm is equivalent to a V_f increase between 1.9% and 7.1%.

An M21E/IMA specimen with the $[45,0, (90,-45)_2,45]_s$ layup (L8), manufactured on a tool with a 4 mm radius, showed a spring-in of 1.56° (increased local V_f). A specimen made on a tool with an 8 mm radius showed a spring-in angle of

1.72°. Thus, the observed V_f inhomogeneity causes maximum spring-in differences of 0.16°.

Two specimens with identical layup, cured on tools with identical radii, but preformed at 40 °C and 60 °C, showed distortion differences of less than 0.02°, which is less than the typical spring-in variation observed for L-profiles manufactured with manual layup [26, 32]. Thus, the spring-in analysis led to the following cognitions.

- No technically relevant, forming-process-related affectation of spring-in magnitudes is identified
- (not related to forming) Smaller tool radii lead to stronger local V_f increases, which in turn results in a reduction of spring-in.

Further tests are desirable and mandatory to substantiate the trends outlined above.

6. Conclusions

Single-diaphragm forming is a cost saving alternative to labor-intensive hand layup. However, adequate forming processes are mandatory to achieve satisfying prepreg-preform quality.

The design of a controlled evacuation-process characteristic was in focus of the present study. It has attracted little attention in available studies on prepreg forming, even though it's a key to high prepreg-preform quality.

The main objective of the presented work was to examine a precisely controlled forming process, which provides a favorable balance between forming speed and prepreg-preform quality.

Hexcel's M21E/IMA prepreg was examined, in order to investigate the effect of its interleaf toughening on the forming process and vice versa. A selected laminate configuration has been manufactured from Hexcel's 8552/AS4 prepreg (no interleaf layers), for sake of comparison.

Forming-induced flaws in the internal laminate architecture and the outer preform appearance were analyzed and correlated with the examined process parameters forming temperature, tool radii and laminate stacking.

Overall, the performed study substantiates that hotforming is capable to manufacture high-quality full-stack prepreg-preforms. The essential outcomes of the performed study are as follows:

- The presented geometrical model shows that the book-end shear angle φ_{shear} only depends on the flange-to-web angle φ_1 of the C profile, which shall be realized by forming $\varphi_{shear} = \arctan\left(\frac{\varphi_1 \cdot \pi}{180°}\right)$. For a 90° flange-to-web angle a shear angle of 57.5° is determined.

---

[3]Note that corner thinning does not occur when profiles are cured with a double-sided tool concept.

- Cure-kinetic analysis shows that even the upper examined forming-temperature threshold of $80\,^{\circ}C$ does not lead to a technically relevant increase of the resin's degree of cure during the analyzed forming periods.
- The presented forming-infrastructure setup allows for precise control of the recipient's pressure profile.
- The analysis of the forming procedure shows that the shear angle develops early on in the forming process. Already a recipient pressure of 50–60 mbar below ambient pressure formed the flat laminates around the tool radii. An additional decrease of the recipient pressure is necessary to fully form the whole laminate onto the tool surface.
- A two-step forming-process characteristic is proposed. Recipient pressure levels of 60 mbar and 510 mbar below ambient pressure were identified as practical. Around two-thirds of the forming-process is allocated for reaching the first pressure level, which addresses the fact that in this period the forming mechanism acts.
- Micro section analysis show that the interleaf layers of the M21E/IMA prepreg are not harmed due to the forming process.
- Analyses of the preform qualities indicate an increase of local fiber waviness for the smallest regarded male-tool radius of 4 mm.
- Comparing forming results of M21E/IMA and 8552/AS4 specimens, with a $[45, 0, (90, -45)_2, 45]_s$ layup, did not reveal clear differences. Higher forming temperatures improved the forming results for both prepregs
- 0.066 mm thick glass-fiber-epoxy-fabric layers (HexPly-M1080), on both laminate-stack surfaces, which are used generally in most series-production prepreg parts for electro-chemical shielding purposes, improve the forming results, as in-plane inter-fiber separation, observed at the laminate-membrane interface is circumvented.
- An affectation of spring-in distortions of cured specimens the forming process was not identified within the present study.
- Overall, the developed forming concept allows for creating prepreg preforms of adequate quality, suitable for series production.

In future research the observed results and indications of the present study will be transferred to more-complex part geometries as investigated by other researchers, in order to assess whether the controlled evacuation process helps to mitigate wrinkling issues.

Disclosure statement

No potential conflict of interest was reported by the authors.

ORCID

E. Kappel 🆔 http://orcid.org/0000-0002-8760-8451

References

[1] Spengler M. Automation der PAG A350 Schalenproduktion. 3 Augsburger Produktionstechnik-Kolloquium, Germany; 2015.
[2] Richardson M. Laying down the fibre-fast! aerospace manufacturing; March 2016.
[3] Lengsfeld H, Wolff-Fabris F, Krämer J, et al. Composite technology: prepregs and monolithic part fabrication technologies. München, Germany: Carl Hanser Verlag; December 2015.
[4] Gillessen A. Continuous high volume part production technologies, 14. Innovation day "Kontinuierliche Profilfertigung", May 2016.
[5] Ott T. Composite hot drape forming. NASA, Washington, Technology 2003: The Fourth National Technology Transfer Conference and Exposition; 1994.
[6] Talreja R, Varna J. Modeling damage, fatigue and failure of composite materials. Amsterdam: Woodhead Publishing, Elsevier; 2016.
[7] Jacob A. Hexcel's composites ready to fly on the A350 XWB. Reinforced plastics; April 2013.
[8] HexCel. HexTow AS4 – product data. HexCel-Composites; September 2009.
[9] HexCel. HexPly 8552 – product data. HexCel-Composites; October 2008.
[10] Gustafson PA, Jastifer JR, Kapenga JA, et al. Lack of statistical rigor in composite materials experimentation and lessons learned from the science of medicine. AIAA/ASME/ASCE/AHS/ASC 55th Structures, Structural Dynamics, and Materials Conference, Maryland, USA; 2014.
[11] Larberg Y. Forming of stacked unidirectional prepreg materials [PhD Thesis]. KTH, Sweden; 2012.
[12] Larberg Y, Åkermo M. On the interply friction of different generations of carbon/epoxy prepreg systems. Comp Part: A. 2011;42(9):1067–1074.
[13] Hallander P, Åkermo M, Mattei C, Pettersson M, et al. An experimental study of mechanisms behind wrinkle development during forming of composite laminates. Compos Part: A. 2013;50: 54–64.
[14] Hallander P, Sjölander J, Åkermo M. Forming induced wrinkling of composite laminates with mixed ply material properties; an experimental study. Compos Part: A. 2015;78:234–245.
[15] Sjölander J, Hallander P, Åkermo M. Forming induced wrinkling of composite laminates: a numerical study on wrinkling mechanisms. Compos Part: A. 2016;81:41–51.
[16] Sun J, Gu Y, Li M, et al. Effect of forming temperature on the quality of hot diaphragm formed C-shaped thermosetting composite laminates. J Reinf Plast Compos. 2012;31(16):1074–1087.

[17] Wang WT, Yu H, Potter K, et al. Improvement of composite drape forming quality by enhancing interply slip. ECCM17 – 17th European Conference on Composite Materials, Munich, Germany; June 2016.

[18] Haanappel S. Forming of UD fibre reinforced thermoplastics – a critical evaluation of intra-ply shear [PhD Thesis]. University of Twente; 2013.

[19] Farnand K, Zobeiry N, Poursartip A, et al. Micro-level mechanisms of fiber waviness and wrinkling during hot drape forming of unidirectional prepreg composites. Compos Part: A. 2017;103: 168–177.

[20] Erland S, Dodwell TJ, Butler R. Characterisation of inter-ply shear in uncured carbon fibre prepreg. Compos Part: A. 2015;77:210–218.

[21] Bian XX, Gu YZ, Sun J, et al. Effects of processing parameters on the forming quality of C-shaped thermosetting composite laminates in hot diaphragm forming process. Appl Compos Mater. 2013;20(5):927–945.

[22] Johnston AA. An integrated model of the development of process-induced deformation in autoclave processing of composite structures [PhD Thesis]. University of British Columbia; 1992.

[23] Hubert P. Aspects of flow and compaction of laminated composite shapes during cure [PhD Thesis]. The University of British Columbia, Vancouver, Canada; May 1996.

[24] Vacuubrand GH. Vacuum controller manual for CVC 3000. PDF documentation; 2017.

[25] Airtech. Low temperature latex rubber bagging material – LRB 100. Data sheet; 2016.

[26] Kappel E. Forced-interaction and spring-in – relevant initiators of process-induced distortions in composite manufacturing. Compos Struct. 2016; 140:217–229.

[27] Li X, Hallett SR, Wisnom MR. Modelling the effect of gaps and overlaps in automated fibre placement (AFP)-manufactured laminates. Sci Eng Compos Mater. 2015;22(2):115–129.

[28] Lan M, Cartie D, Davies P, Baley C. Influence of embedded gap and overlap fiber placement defects on the microstructure and shear and compression properties of carbon? Epoxy laminates. Compos Part: A. 2016;82:198–207.

[29] Sawicki AJ, Minguet PJ. The effect of intraply overlaps and gaps upon the compression strength of composite laminates. 39th AIAA/ASME/ASCE/ AHS/ASC Structures, Structural Dynamics, and Materials Conference and Exhibit Long Beach, USA' 1998.

[30] HexCel. HexPly M21 – product data. HexCel-Composites; March 2010.

[31] Hubert P, Poursartip A. Aspects of the compaction of composite angle laminates: An experimental investigation. J Compos Mater. 2001; 35(1):2–26.

[32] Kappel E. Process distortions in composite manufacturing - from an experimental characterization to a prediction approach for the global scale [PhD Thesis]. Otto-von-Guericke University Magdeburg, Germany; 2013.